THE JOURNAL OF BIOLOGICAL CHEMISTRY

Vol. 274, No. 5, Issue of January 29, pp. 2706–2716, 1999
Printed in U.S.A.

Poliovirus RNA-dependent RNA Polymerase ($3D^{pol}$) Is Sufficient for Template Switching *in Vitro**

(Received for publication, July 16, 1998, and in revised form, November 4, 1998)

Jamie J. Arnold and Craig E. Cameron‡

From the Department of Biochemistry and Molecular Biology, Pennsylvania State University, University Park, Pennsylvania 16802

We have performed a systematic, quantitative analysis of the kinetics of nucleotide incorporation catalyzed by poliovirus RNA-dependent RNA polymerase, $3D^{pol}$. Homopolymeric primer/templates of defined length were used to evaluate the contribution of primer and template length and sequence to the efficiency of nucleotide incorporation without the complication of RNA structure. Interestingly, thermodynamic stability of the duplex region of these primer/templates was more important for efficient nucleotide incorporation than either primer or template length. Surprisingly, products greater than unit length formed in all reactions regardless of length or sequence. Neither a distributive nor a processive slippage mechanism could be used to explain completely the formation of long products. Rather, the data were consistent with a template-switching mechanism. All of the nucleotide could be polymerized during the course of the reaction. However, very few primers could be extended, suggesting an inverse correlation between the efficiency of primer utilization and that of nucleotide incorporation. Therefore, the greatest fraction of incorporated nucleotide derives from a small fraction of enzyme when radioactive nucleotide and homopolymeric primer/template substrates are employed. The impact of these results on mechanistic studies of $3D^{pol}$-catalyzed nucleotide incorporation and RNA recombination are discussed.

Positive-strand RNA viruses cause a variety of diseases in humans ranging from the common cold (1) to chronic hepatitis (2). Critical to the replication of the genomes of these viruses is the virus-encoded, RNA-dependent RNA polymerase (RdRP)[1] (3). As this enzymatic activity is unique to virus-infected cells, the viral RdRP represents a very attractive target for the design of antiviral agents to treat RNA virus infection. Most positive-strand RNA viruses are thought to have the same general replication strategy, and this belief is generally extended to include the mechanism of genome replication (3). RdRPs from many viruses have been characterized to some extent (3–9). However, in no instance is detailed, mechanistic information available. This fact is even true for viruses, such as poliovirus, for which genetic and biochemical systems to study genome replication have existed for many years (10).

Notwithstanding, poliovirus is one of the best understood systems with respect to the biochemistry of genome replication and is, therefore, an invaluable paradigm for all positive-strand RNA viruses (10). Replication of poliovirus genome initiates within the poly(A)-tract at the 3′-end of genomic RNA from a complex comprising viral factors (3AB, 3CD, 3B, and $3D^{pol}$) (11–13) and possibly cellular factors (14). 3AB and 3CD are required primarily to establish an initiation complex, possibly by recruiting the polymerase, $3D^{pol}$ (13). 3AB is a RNA-binding protein capable of interacting with $3D^{pol}$ (15,16) that possibly stimulates the rate of elongation of nascent RNA (17) or enhances the efficiency of primer utilization (18). RNA synthesis is catalyzed by $3D^{pol}$, which initiates RNA synthesis from the protein primer, 3B. 3B is most often referred to as VPg.

The recent solution of the crystal structure of poliovirus RdRP by the Schultz laboratory has catapulted this enzyme, in terms of structure, to the level of the other classes of nucleic acid polymerase (19). Thus, a more precise understanding of the structure-function relationships of this enzyme is now possible. To be sure, an understanding of the elementary steps employed by polymerases in catalyzing nucleotide incorporation is essential in order to evaluate accurately the effects of mutations. Unfortunately, the prevailing absence of detailed, mechanistic information for $3D^{pol}$ greatly limits the extent to which the structural information can be exploited. This is due, primarily, to the inability to establish stoichiometric complexes between $3D^{pol}$, primer/template, and nucleotide.

In this report, we have performed a systematic, quantitative analysis of the kinetics of $3D^{pol}$-catalyzed nucleotide incorporation using homopolymeric substrates of defined length. These studies provide insight into the properties of primer/template required for the assembly of stoichiometric complexes between $3D^{pol}$ and primer/template. This information should prove useful in the design of heteropolymeric primer/templates to elaborate a detailed kinetic mechanism for this enzyme and, perhaps, other RdRPs. In addition, these studies revealed the unexpected ability of poliovirus $3D^{pol}$ alone to undergo template switching *in vitro*.

EXPERIMENTAL PROCEDURES

Materials

[α-^{32}P]GTP (>3,000 Ci/mmol) and [α-^{32}P]UTP (>6,000 Ci/mmol) were from NEN Life Science Products; [γ-^{32}P]ATP (>7,000 Ci/mmol) was from ICN; nucleoside 5′-triphosphates and poly(rA) were from Amersham Pharmacia Biotech; poly(rC) and heparin 6000 were from Sigma; all DNA oligonucleotides were from Operon Technologies, Inc. (Alameda, CA); all RNA oligonucleotides were from Dharmacon Research, Inc. (Boulder, CO); T4 polynucleotide kinase was from New England Biolabs; single-stranded 10-nucleotide ladder was from Life Technologies, Inc.; 2.5-cm DE81 filter paper discs were from Whatman. All other reagents were of the highest grade available from Sigma or Fisher.

* This work was supported in part by Howard Temin Award CA75118 from the NCI, National Institutes of Health (to C. E. C.). The costs of publication of this article were defrayed in part by the payment of page charges. This article must therefore be hereby marked "*advertisement*" in accordance with 18 U.S.C. Section 1734 solely to indicate this fact.

‡ To whom correspondence should be addressed. Tel.: 814-863-8705; Fax: 814-863-7024; E-mail: cec9@psu.edu.

[1] The abbreviations used are: RdRP, RNA-dependent RNA polymerase; PAGE, polyacrylamide gel electrophoresis; nt, nucleotide(s).

Expression and Purification of 3D^{pol}

Construction of the plasmid directing the expression of 3D^{pol} with an authentic, glycine amino terminus and the details of purification will be described elsewhere.[2] Briefly, the plasmid contains a gene encoding a ubiquitin-3D^{pol} fusion protein under control of the bacteriophage T7 RNA polymerase promoter (20). *Escherichia coli*, BL21(DE3), co-transformed with the 3D^{pol} expression plasmid and plasmid pCG1, which directs the expression of a ubiquitin protease (20), were grown to A_{600} = 0.8 in NZCYM medium (Life Technologies, Inc.), and expression was induced by addition of isopropyl-1-thio-β-D-galactopyranoside to 500 μM. Cells were harvested by centrifugation after 4 h. 3D^{pol} was purified to greater than 95% purity by using a combination of ammonium sulfate precipitation and phosphocellulose (Whatman), S-Sepharose (Amersham Pharmacia Biotech), and Q-Sepharose (Amersham Pharmacia Biotech) chromatographies as described previously (5, 6, 19). The final preparation was concentrated to 468 μM by using a second Q-Sepharose column. The protein concentration was determined by Bio-Rad protein assay using bovine serum albumin (Pierce) as a reference.

Purification of Synthetic Oligonucleotides

DNA and RNA oligonucleotides were purified by denaturing PAGE. Gels consisted of: 18% acrylamide, 2% bisacrylamide, 7 M urea, and 1× TBE (89 mM Tris base, 89 mM boric acid, and 2 mM EDTA). The oligonucleotide ladder was visualized by UV shadowing. A gel slice containing only the full-length oligonucleotide was removed, and the nucleic acid was electroeluted from the gel in 1× TBE by using an Elutrap apparatus (Schleicher & Schuell). Oligonucleotides were desalted on Sep-Pak columns (Millipore) as specified by the manufacturer. Oligonucleotides were typically suspended in TE (10 mM Tris, 1 mM EDTA, pH 8.0), aliquoted, and stored at −80 °C until use. Concentrations were determined by measuring the absorbance at 260 nm by using calculated extinction coefficients (21).

Purity of [α-^{32}P]NTPs

[α-^{32}P]NTPs were diluted to 0.1 μCi/μl in distilled, deionized H_2O, and 1 μl was spotted in triplicate onto polyethyleneimine-cellulose TLC plates (EM Science). TLC plates were developed in 0.3 M potassium phosphate, pH 7.0, dried, and exposed to a PhosphorImager screen. Imaging and quantitation were performed by using the ImageQuant software from Molecular Dynamics. The purity was used to correct the specific activity of NTP in reactions in order to calculate accurate concentrations of product. Purity was checked before or after each experiment and ranged from 50% to 90%.

5′-^{32}P Labeling of Oligonucleotides

DNA and RNA oligonucleotides were end-labeled by using [γ-^{32}P]ATP and T4 polynucleotide kinase essentially as specified by the manufacturer. Reactions typically contained 11 μM [γ-^{32}P]ATP, 10 μM DNA or RNA oligonucleotide, and 0.4 units/μl T4 polynucleotide kinase. Unincorporated nucleotide was removed by passing the sample over two consecutive 1-ml Sephadex G-25 (Sigma) spun columns.

5′-^{32}P Labeling of DNA Ladder

Labeling of the DNA ladder was performed by using [γ-^{32}P]ATP and T4 polynucleotide kinase as specified by Life Technologies, Inc.

3D^{pol} Assays

Reactions contained 50 mM HEPES, pH 7.5, 10 mM 2-mercaptoethanol, 5 mM $MgCl_2$, 60 μM $ZnCl_2$, 0.2 μCi/μl [α-^{32}P]NTP, 500 μM NTP, primer/template, and 3D^{pol}. Reactions were quenched by the addition of EDTA to a final concentration of 50 mM. Specific concentrations of primer/template and 3D^{pol}, along with any deviations from the above, are indicated in the appropriate figure legend.

Product Analysis

DE81 Filter Binding—10 μl of the quenched reaction was spotted onto DE81 filter paper discs and dried completely. The discs were washed three times for 10 min in 250 ml of 5% dibasic sodium phosphate and rinsed in absolute ethanol. Bound radioactivity was quantitated by liquid scintillation counting in 5 ml of Ecoscint scintillation fluid (National Diagnostics).

Denaturing PAGE—10 μl of the quenched reaction mixture was added to an equal volume of loading buffer (80% formamide, 100 mM EDTA, 50 mM Tris borate, 0.15% bromphenol blue, and 0.15% xylene cyanol) and heated to 70 °C for 1 min prior to loading 5 μl on a 1× TBE polyacrylamide gel of the appropriate percentage. Electrophoresis was performed in 1× TBE at 30 mA. Gels were visualized and quantitated by using a PhosphorImager.

RESULTS

Primer Length and Sequence Composition Modulate the Rate of 3D^{pol}-catalyzed Nucleotide Incorporation—The ability to identify the individual steps employed by 3D^{pol} during a single cycle of nucleotide incorporation requires the assembly of stoichiometric complexes between 3D^{pol} and substrates: primer/template and nucleotide. Formation of such complexes with DNA-dependent DNA polymerases and reverse transcriptases is an ordered process with primer/template binding prior to nucleotide (22–26). In addition, stability of the initial binary complex depends on the length of primer/template, and rate of nucleotide incorporation depends on sequence (22). In order to evaluate rapidly the effect of primer and template length and sequence composition on the efficiency of nucleotide incorporation catalyzed by 3D^{pol}, without the complication of nucleic acid structure, we have used combinations of a variety of homopolymeric oligonucleotides and polynucleotides of defined length as primer/template substrates for 3D^{pol}.

In the first series of experiments, poly(rA) was used as template and DNA oligonucleotides ranging in size from 6 to 20 nt were used as primers (Fig. 1*A*). As reported previously, *de novo* synthesis is not observed on poly(rA) (27). However, 3D^{pol}-catalyzed nucleotide incorporation was observed with oligo(dT) primers 6 nt or longer (Fig. 1*A*). In addition, a primer length of 15–20 nt was optimal for most efficient nucleotide incorporation (Fig. 1*A*). By using a 15- or 20-nt oligo(dT) primer, the amount of product formed was increased 5–25-fold relative to that observed with either a 6- or 10-nt primer. This apparent effect of primer length on 3D^{pol}-catalyzed nucleotide incorporation was not due to changes in the fraction of template coated by primer as this ratio was constant. In each case, a primer concentration sufficient to coat 30% of the template was used. It is worth noting, however, that maximal rates of nucleotide incorporation were observed only when a primer concentration sufficient to coat 30–100% of the template was used (Fig. 2).

When a similar series of experiments was performed using poly(rC) as template, *de novo* synthesis was observed, albeit at a 5–10-fold lower efficiency relative to that observed in the presence of a primer (Fig. 1*B*). In contrast to oligo(dT)-primed poly(rU) synthesis, a 6-nt oligo(dG) primer was optimal for most efficient poly(rG) synthesis (Fig. 1*B*). Moreover, a 2-fold decrease in the amount of nucleotide incorporated was noted as the length of the primer was increased to 10 nt (Fig. 1*B*). The level of nucleotide incorporation was essentially the same for oligo(dG) primers 10, 15, or 20 nt in length (Fig. 1B). Experiments were also performed using 15-nt oligo(rU) and oligo(rG) primers. No significant difference in activity was observed with these RNA primers relative to the corresponding 15-nt DNA primers (data not shown).

In order to assess more directly the effects of primer and template length on the efficiency of nucleotide incorporation, steady-state kinetic analysis was performed on the following primer/templates: dT_{15}/rA_{400}, dT_{15}/rA_{30}, dT_{15}/rA_{16}, and dT_{10}/rA_{16}; the data are presented in Table I. The K_m values varied from 24.6 μM (dT_{15}/rA_{30}) to 122 μM (dT_{10}/rA_{16}), and the V_{max} values varied from 1.1 μM/min (dT_{15}/rA_{16}) to 13.1 μM/min (dT_{15}/rA_{400}). Although no change in the K_m for primer/template was observed when the length of the template was changed from 400 to 16 nt, a 3–5-fold increase in the K_m was observed by changing the primer length from 15 to 10 nt. Interestingly, even under conditions of saturating substrates, the kinetics of nucleotide incorporation varied from substrate to substrate

[2] D. W. Gohara, J. J. Arnold, and C. E. Cameron, manuscript in preparation.

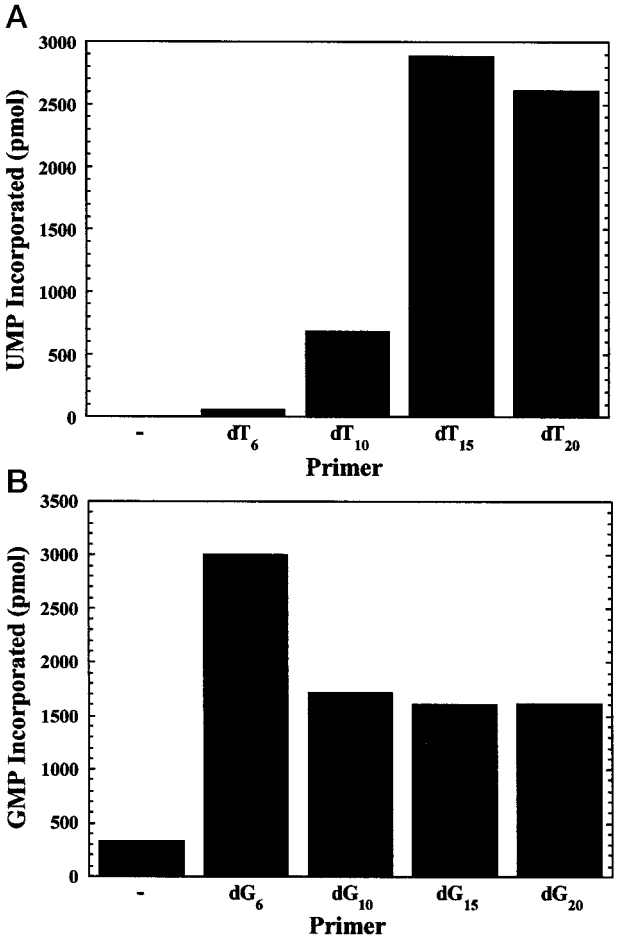

FIG. 1. **Primer length and sequence composition modulate the rate of 3D^{pol}-catalyzed nucleotide incorporation.** *A*, reactions contained 0.5 μM 3D^{pol}, 0.2 μM poly(rA) (93.4 μM AMP), UTP (500 μM), and oligo(dT)$_n$ (where n = 6, 10, 15, or 20) sufficient to coat 30% of the template ([AMP]/[TMP] = 3.33). Reactions were initiated by addition of 3D^{pol} and incubated at 37 °C for 5 min. The reaction volume was 50 μl. *B*, reactions were performed as described above with poly(rC), oligo(dG)$_n$, and GTP.

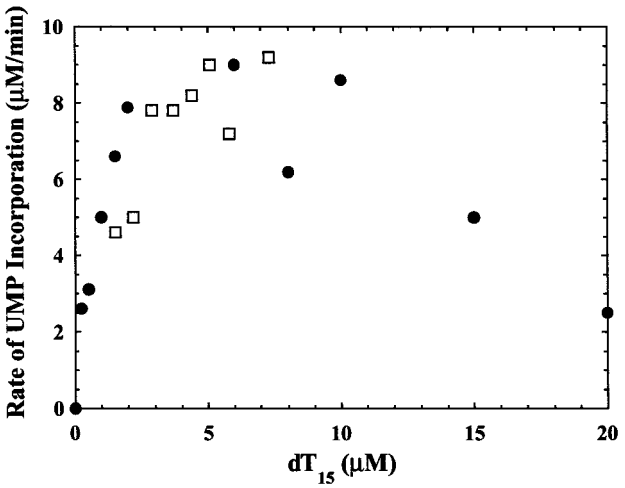

FIG. 2. **An optimal primer:template ratio exists for maximal rates of 3D^{pol}-catalyzed nucleotide incorporation.** Reactions contained 3D^{pol} (0.5 μM), poly(rA) (60 μM AMP), UTP (20 μM), and dT$_{15}$ (0–20 μM). Reactions were initiated by addition of 3D^{pol} and incubated at 37 °C for 5 min. The different symbols represent two individual experiments.

TABLE I
Steady-state kinetic analysis of dT$_n$/rA$_n$ primer/templates

Time courses of nucleotide incorporation in reactions containing 3D^{pol} (0.5 μM) and dT$_n$/rA$_n$ (1–200 μM) were obtained. The reaction rate at each primer/template concentration was determined by linear regression and plotted as a function of primer/template concentration. The data were fit to a hyperbola to obtain values for K_M and V_{max}.

Primer/template	K_M	V_{max}
	μM	$\mu M/min$
dT$_{15}$/rA$_{400}$	45.3 ± 10.4	13.1 ± 1.5
dT$_{15}$/rA$_{30}$	24.6 ± 2.8	9.1 ± 0.5
dT$_{10}$/rA$_{16}$	122 ± 44	4.8 ± 0.9
dT$_{15}$/rA$_{16}$	38.2 ± 8.5	1.1 ± 0.1

(Fig. 3). Both the duration of linearity and the reaction end points differed substantially when the kinetics of nucleotide incorporation into dT$_{15}$/rA$_{16}$ (Fig. 3*A*) was compared with that into dT$_{15}$/rA$_{30}$ (Fig. 3*B*) or dG$_{15}$/rC$_{30}$ (Fig. 3*C*). The K_m of 3D^{pol} for dG$_{15}$/rC$_{30}$ is in the 15 μM range (data not shown). Therefore, in order to ensure accurate measurement of reaction rates as a function of substrate or enzyme concentration, reaction rates were determined from the linear phase of complete time courses.

When the dependence of the reaction rate on enzyme concentration was measured using the linear phase of complete time courses, no evidence was obtained to support the hypothesis that oligomerization of 3D^{pol} is necessary for activity as suggested by Pata *et al.* (28). Fig. 4*A* shows the linear phase of time courses for reactions under conditions of saturating substrates using concentrations of 3D^{pol} ranging from 0.5 μM to 2.0 μM. A plot of reaction rates, obtained by linear regression of the data shown in Fig. 4*A*, as a function of 3D^{pol} concentration showed a linear relationship. Therefore, the cooperative transition in the 0.5–2.0 μM range observed by Pata *et al.* (28) may be a reflection of the "snap-back" RNA substrate employed in that study. Finally, the dependence of the rate of nucleotide incorporation on 3D^{pol} concentration was also linear in the 0.05–5 μM range (data not shown).

Products Greater than Unit Length Form Using dT$_{15}$/rA$_{16}$, dT$_{15}$/rA$_{30}$, and dG$_{15}$/rC$_{30}$ Primer/Templates—It has been reported by several investigators studying the oligo(dT)-primed, poly(rU)-polymerase activity of 3D^{pol} that this enzyme extends, at best, 0.1–1% of primers in reactions which typically contain a concentration of primer in the 1 μM range (28, 29). Such a low fraction of primer utilization is not surprising, however, given a K_m of 3D^{pol} for dT$_{15}$/rA$_{400}$ of 45 μM. Therefore, it was comforting to note that the concentration of UMP incorporated was almost stoichiometric with respect to primer under saturating conditions of dT$_{15}$/rA$_{16}$ (Fig. 3*A*). This suggested that in this reaction a greater fraction of primers were utilized. However, when products of reactions employing an end-labeled, (dT)$_{15}$ primer were resolved by denaturing PAGE and visualized by phosphorimaging, extended primer was not observed (data not shown).

In order to increase the limit of detection, products of reactions employing [α-^{32}P]UTP were resolved by denaturing PAGE and visualized by phosphorimaging. Surprisingly, products ranging in length from 16 to 300 nt were apparent (data not shown). In order to verify that the origin of the long products was not contaminating nucleic acid, an experiment was performed in which 2 μM 3D^{pol}, 122 μM dT$_{15}$/rA$_{16}$, and 0.5 μM [α-^{32}P]UTP were incubated at 37 °C for 30, 60, or 90 s and then either quenched by the addition of EDTA or chased by the addition of 1000-fold molar excess of UTP and quenched after 10 min. Products were resolved by denaturing PAGE and visualized by phosphorimaging (Fig. 5). The pulse-quench experiment showed that the only products formed were those consistent with utilization of the 15-nt oligo(dT) primer. Moreover,

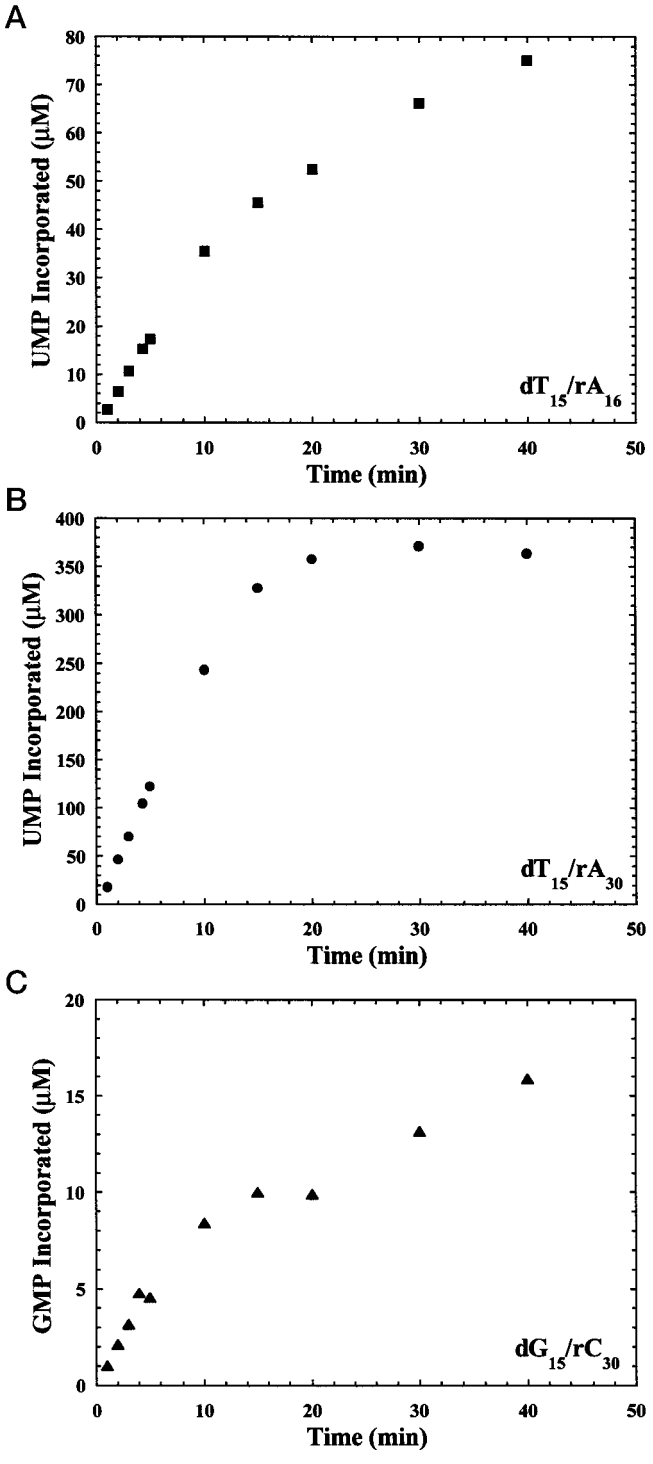

FIG. 3. **Kinetics of nucleotide incorporation by 3D^{pol} are substrate-dependent.** *A*, time course for nucleotide incorporation with dT_{15}/rA_{16}. Reaction contained 3D^{pol} (2 μM) and dT_{15}/rA_{16} (122 μM). Reaction was initiated by addition of 3D^{pol} and incubated at 37 °C. *B*, time course for nucleotide incorporation with dT_{15}/rA_{30} (122 μM). *C*, time course for nucleotide incorporation with dG_{15}/rC_{30} (122 μM).

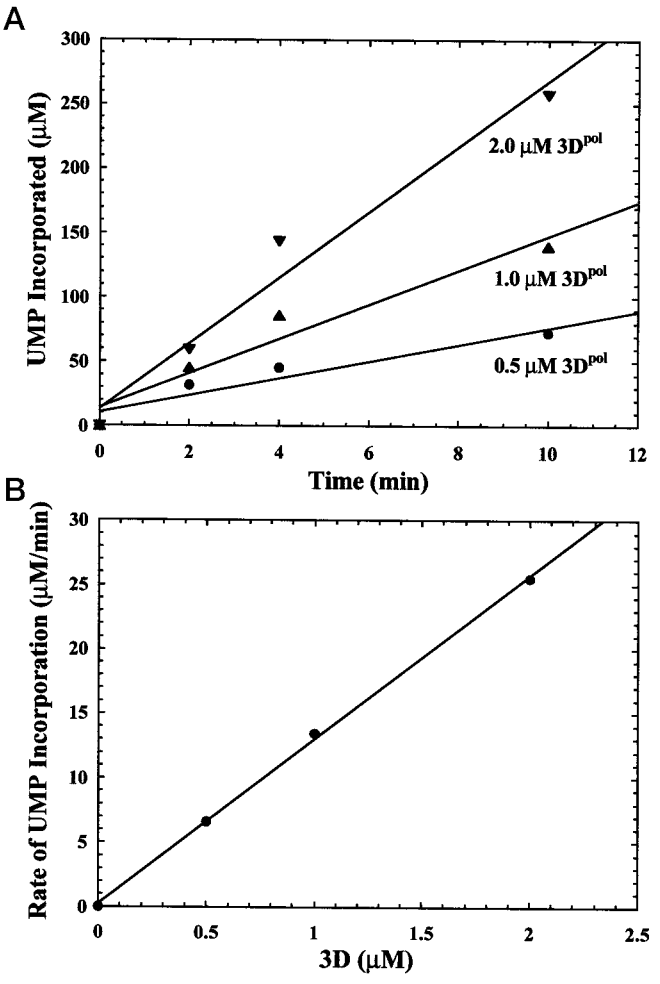

FIG. 4. **The rate of nucleotide incorporation exhibits a linear dependence on 3D^{pol} concentration.** *A*, time course for nucleotide incorporation with dT_{15}/rA_{30} (122 μM) using 0.5, 1.0, or 2.0 μM 3D^{pol}. Reaction was initiated by addition of 3D^{pol} and incubated at 37 °C. *B*, rate of nucleotide incorporation (as determined from linear regression of time courses in *A*) plotted as a function of 3D^{pol} concentration.

the products labeled in the pulse were chased into the longer products (Fig. 5).

The ability to form products greater than unit length was not unique to the dT_{15}/rA_{16} primer/template. Long products were observed with dT_{15}/rA_{30} and dG_{15}/rC_{30} primer/templates (Fig. 6). The efficiency of formation of products greater than unit length was sensitive to sequence composition. The magnitude of label incorporated into products from the dG_{15}/rC_{30} reaction was reduced by an order of magnitude relative to that from the dT_{15}/rA_{30} reaction (*cf.* Fig. 3, *B* and *C*).

Models for Formation of Products Greater than Unit Length—Because previous studies of 3D^{pol} employing long, homopolymeric substrates appeared to produce unit-length products (5, 6, 17), the formation of products greater than unit length on short, homopolymeric substrates was not expected. However, this phenomenon has been reported for most classes of nucleic acid polymerase studied to date. Several mechanisms have been proposed to explain formation of these products (30–33), and three possible mechanisms are illustrated in Fig. 7. The first possibility is a distributive slippage mechanism (Fig. 7, *i*) in which the polymerase dissociates from primer/template, the primer terminus realigns relative to template, and enzyme rebinds and extends. Several iterations of this pathway would yield products greater than unit length. A second possibility is a processive slippage mechanism (Fig. 7, *ii*). Again, realignment of the primer occurs relative to template; however, polymerase does not dissociate. Finally, template switching (copy-choice recombination) may be the mechanism of formation of products greater than unit length (Fig. 7, *iii*). Polymerase, in complex with nascent chain, dissociates from template (donor) and binds to another (acceptor). A permutation of this mechanism would require polymerase to reach the end of template for efficient template switching to occur

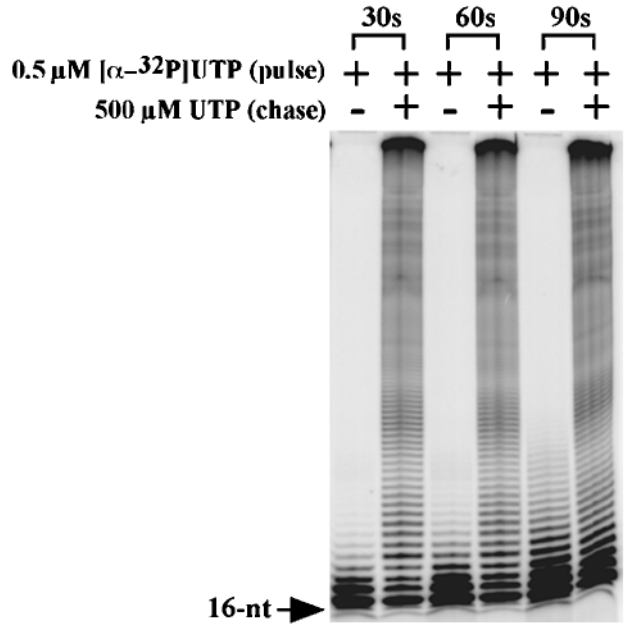

FIG. 5. **Primer-dependent products that are greater than unit length form by using dT_{15}/rA_{16}.** Reaction contained 3D^{pol} (2 μM), dT_{15}/rA_{16} (122 μM), and 0.5 μM [α-^{32}P]UTP. Reactions were initiated by addition of 3D^{pol} and incubated at 37 °C for 30, 60, or 90 s (pulse), at which time the reactions were either quenched by addition of EDTA or chased by addition of UTP to 500 μM and incubation continued an additional 10 min. Products were resolved by electrophoresis on a denaturing 15% polyacrylamide gel.

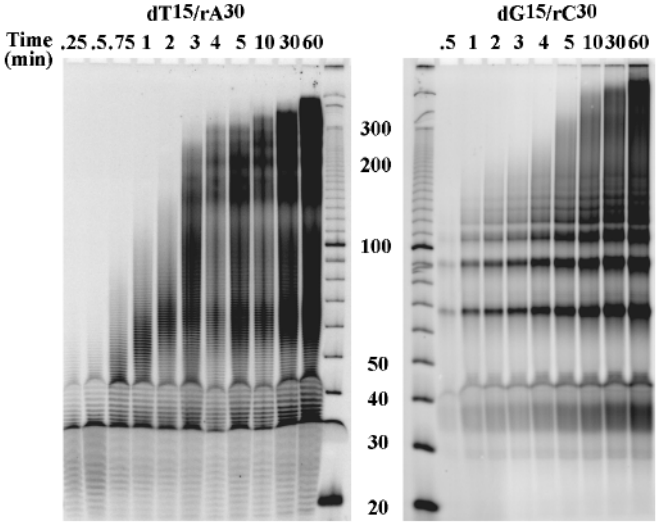

FIG. 6. **Long products are observed with dT_{15}/rA_{30} and dG_{15}/rC_{30} primer/templates.** Reaction contained 3D^{pol} (0.5 μM) and dT_{15}/rA_{30} (10 μM) or dG_{15}/rC_{30} (10 μM). Reactions were initiated by addition of 3D^{pol} and incubated at 37 °C. Products were resolved by electrophoresis on a denaturing 8% polyacrylamide gel. The size of selected bands from the single-stranded DNA ladder is indicated as a reference.

(forced-copy-choice recombination). Although template switching via a copy-choice mechanism could occur before, during, or after polymerase reaches the end of template, template switching would occur most frequently once polymerase reaches the end of donor template via a forced copy-choice mechanism. While a distributive slippage mechanism has been proposed for DNA polymerase I to explain formation of long products from short primer/templates consisting of 3-nt repeats (33), a processive slippage mechanism has been suggested for T7 DNA polymerase on the same substrates (33). In the case of the

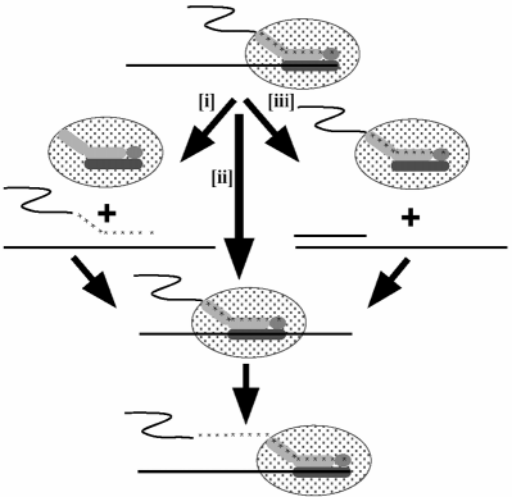

FIG. 7. **Models for long product formation: *i*, distributive slippage; *ii*, processive slippage; *iii*, template switching.** See text for details.

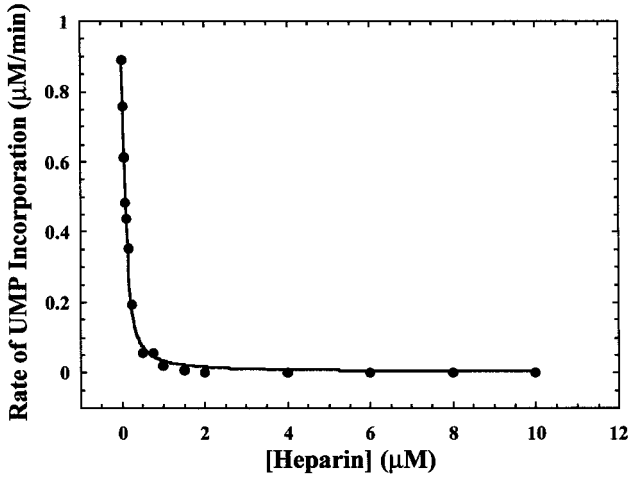

FIG. 8. **3D^{pol} is inhibited by heparin.** Reaction contained 3D^{pol} (0.28 μM), poly(rA) (60 μM AMP), dT_{15} (1.5 μM), UTP (20 μM), and heparin 6000 (0–10 μM). Reaction was initiated by addition of 3D^{pol} and incubated at 37 °C for 10 min. The *solid line* represents the fit of the data to the quadratic equation that gives a K_i for heparin 6000 of 33 ± 4.5 nM.

reverse transcriptases from avian myeloblastosis virus (30, 31) and human immunodeficiency virus (32), a template-switching mechanism has been proposed to explain products greater than unit length on a poly(rA) template.

Formation of Products Greater than Unit Length Does Not Occur by a Distributive or Processive Slippage Mechanism—As slippage was a very probable explanation for formation of long products, our initial experiments were designed to distinguish between a distributive and a processive slippage mechanism. If slippage were occurring by a distributive mechanism, then long products should not form in the presence of a trap for free enzyme. In contrast to results obtained with the encephalomyocarditis 3D^{pol} (34), heparin is a very effective inhibitor of poliovirus 3D^{pol} with a K_i in the 30 nM range (Fig. 8). When a reaction containing dT_{15}/rA_{30} primer/template, [α-^{32}P]UTP, and heparin was initiated by addition of poliovirus polymerase, a significant level of nucleotide incorporation was not observed during a 60 min incubation period (Fig. 9*A*, *Pre-Trap*). However, when polymerase and primer/template were incubated for 5 min at 37 °C, and the reaction initiated by addition of

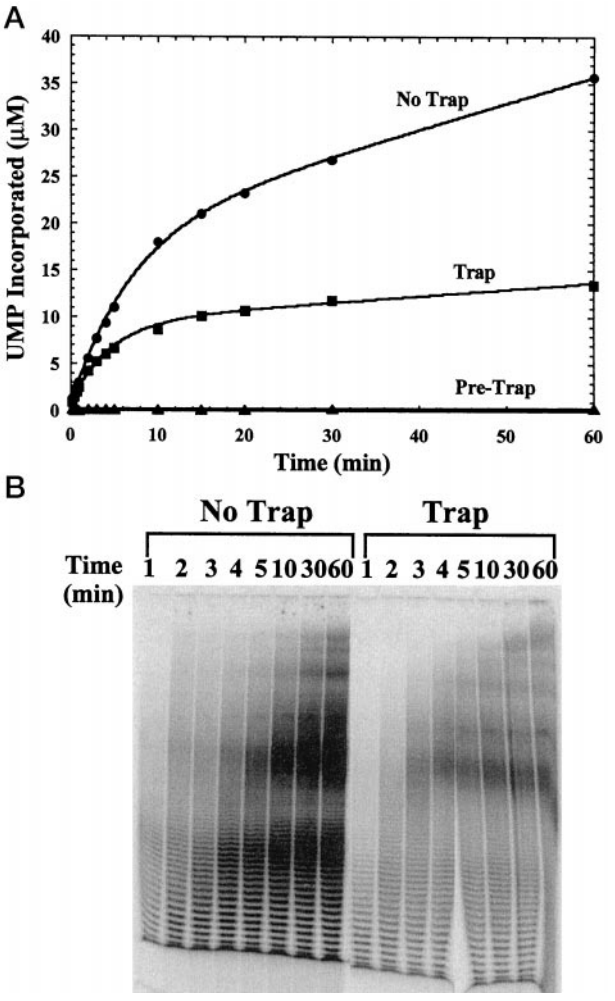

FIG. 9. **Heparin-resistant complexes produce long products.** *A*, reactions contained 3D^{pol} (0.5 μM) and dT_{15}/rA_{30} (20 μM), with or without heparin 6000 (100 μM). 3D^{pol} was incubated with dT_{15}/rA_{30} at 37 °C for 1 min and the reaction was initiated by addition of UTP (●, *No Trap*) or UTP and heparin (■, *Trap*). In the control experiment (▲), *Pre-Trap*), heparin was included during the initial incubation and the reaction initiated by addition of UTP. *B*, reaction products resolved by electrophoresis on a denaturing 10% polyacrylamide gel.

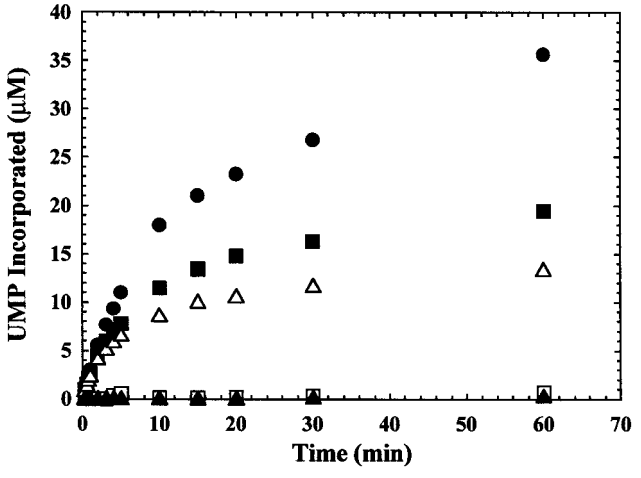

FIG. 10. **Heparin concentration modulates the activity of "heparin-resistant" complexes.** Reactions contained 3D^{pol} (0.5 μM), dT_{15}/rA_{30} (20 μM), and heparin 6000 (0, 10, or 100 μM). 3D^{pol} was incubated with dT_{15}/rA_{30} at 37 °C for 1 min, and the reaction was initiated by addition of UTP (●), UTP and 10 μM heparin (■), or UTP and 100 μM heparin (△). In the control experiments, heparin was included during the initial incubation at either 10 μM (□) or 100 μM (▲) and the reaction initiated by addition of UTP.

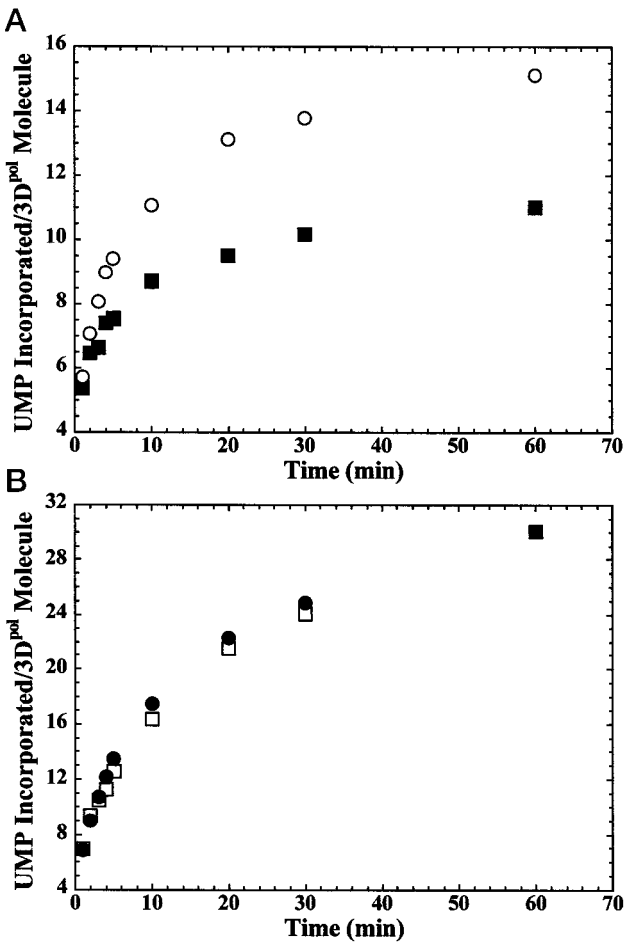

FIG. 11. **Nucleotide incorporated per 3D^{pol} molecule is diminished by dilution.** *A*, reactions were initiated by mixing 3D^{pol} (5 μM), dT_{15}/rA_{30} (10 μM), UTP (500 μM), and [α-^{32}P]UTP (0.2 μCi/μl) and incubated at 30 °C for 3 min, at which time reactions were diluted such that UTP concentration was not changed, heparin was added to a final concentration of 10 μM, and the final concentrations of 3D^{pol} and dT_{15}/rA_{30} were either 0.5 μM 3D^{pol} and 1 μM dT_{15}/rA_{30} (○) or 0.1 μM 3D^{pol} and 0.2 μM dT_{15}/rA_{30} (■). After dilution, reactions were quenched at the indicated times by addition of EDTA to a final concentration of 50 mM. *B*, reactions were performed as described above; however, the diluted reactions were supplemented with rA_{30} acceptor template to a final concentration of 100 μM.

[α-^{32}P]UTP and heparin, the initial rate of nucleotide incorporation was unchanged relative to a reaction performed in the absence of trap (Fig. 9A, *cf. Trap* and *No Trap*). The reaction terminated prematurely relative to that in the absence of trap; therefore, products most likely result from complexes that assembled during preincubation. Analysis of reaction products by phosphorimaging after denaturing PAGE indicated that long products formed in the presence of heparin, *i.e.* without dissociation of polymerase (Fig. 9*B*). These data are consistent with a processive slippage mechanism.

Interestingly, complexes that were competent to form long products were also sensitive, to some extent, to inhibition by heparin albeit at a substantially higher concentration than that for free enzyme. Although both 10 μM heparin and 100 μM heparin were sufficient to trap free enzyme, the rate of the second phase of the reaction was inhibited to a greater extent by 100 μM heparin than by 10 μM heparin (Fig. 10). This observation may suggest that complexes that form long products can exist in a form that is not "free" but is accessible to heparin. Such a complex might be expected if template switching occurred.

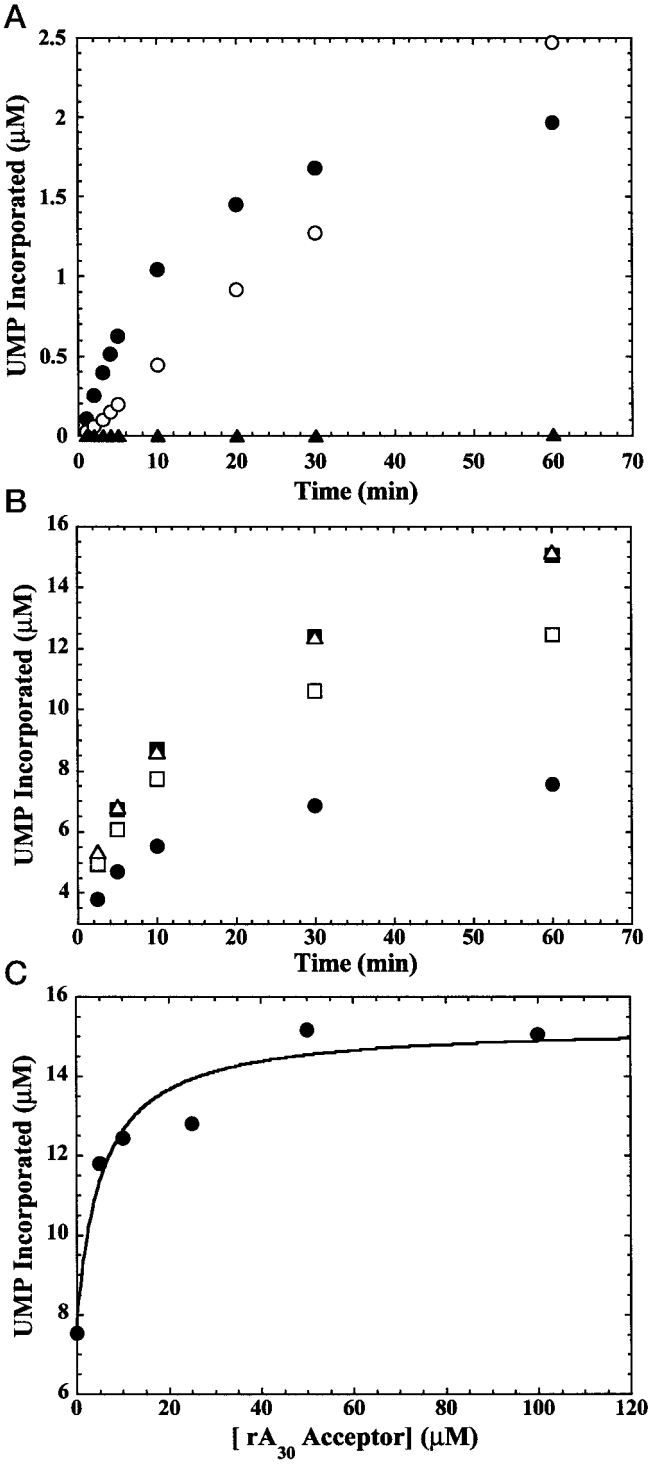

FIG. 12. **Nucleotide incorporated by 3D^{pol} is stimulated by acceptor template.** *A*, reactions contained 0.5 μM 3D^{pol}, 1 μM dT_{15}/rA_{30}, and either 0 μM rA_{30} and 0 μM heparin (●), 100 μM rA_{30} and 0 μM heparin (○), or 100 μM rA_{30} and 10 μM heparin (▲). Reactions were initiated by addition of 3D^{pol} and incubated at 30 °C. *B*, 3D^{pol} (5 μM), dT_{15}/rA_{30} (10 μM), UTP (500 μM), and [α-^{32}P]UTP (0.2 μCi/μl) were incubated at 30 °C for 3 min, at which time reactions were diluted such that the final concentrations of 3D^{pol} and dT_{15}/rA_{30} were 0.5 and 1 μM, respectively, UTP concentration was not changed, heparin was added to a final concentration of 10 μM, and rA_{30} acceptor template was added to a final concentration of 0 μM (●), 10 μM (□), 50 μM (△), or 100 μM (■). After dilution, reactions were quenched at the indicated times by addition of EDTA to a final concentration of 50 mM. *C*, UMP incorporated as a function of rA_{30} acceptor template concentration obtained from reactions as described in *B*. The *solid line* represents the fit of the data to a hyperbola with a $K_{0.5}$ for rA_{30} acceptor of 5.4 ± 2.6 μM.

In order to test the processive slippage mechanism directly, the following experiment was performed. Polymerase (5 μM), dT_{15}/rA_{30} (10 μM), and UTP/[α-^{32}P]UTP (500 μM) were incubated at 30 °C for 3 min to assemble stable elongation complexes and initiate RNA synthesis. The elongating complexes were then diluted into reactions containing heparin (10 μM) such that the complexes were diluted 10- or 50-fold. Thus, in one reaction, the final concentrations of polymerase and primer/template were 0.5 and 1 μM, respectively; in the other, the final concentrations of polymerase and primer/template were 0.1 and 0.2 μM, respectively. Heparin was added to the reaction in order to preclude reinitiation. Please note that the *x* axis (time) in this experiment and subsequent experiments represents time after the initial 3-min incubation. Therefore, at t = 0 the product formed is that formed during the initial 3-min incubation. Because processive slippage is a first order process, this reaction should be insensitive to dilution. Product formed per molecule of polymerase should be independent of polymerase and primer/template concentration if polymerase-primer/template-nucleotide complexes are preformed. As shown in Fig. 11*A*, this was not the case. The reaction was sensitive to dilution. In order to demonstrate directly that the diminution in the amount of product formed per molecule of polymerase observed upon dilution was a consequence of a reduction in the concentration of acceptor RNA rather than dissociation of polymerase-primer/template complexes, we performed the experiment described above and supplemented the diluted reaction mixtures with acceptor RNA. As shown in Fig. 11*B*, product formed per molecule of polymerase was unchanged, thus confirming that the primary effect of dilution in the experiment shown in Fig. 11*A* was a reduction in the concentration of acceptor RNA. Taken together, these data are consistent with a bimolecular reaction, such as template switching, contributing to formation of long products.

Template Switching Is the Primary Pathway for Formation of Products Greater than Unit Length—The use of a template-switching mechanism by 3D^{pol} to produce products greater than unit length would be supported further by demonstrating a dependence of the reaction rate on the concentration of acceptor template (rA_{30}) (31, 32). The presence of acceptor template in reactions prior to assembly was inhibitory (Fig. 12*A*), and concentrations of acceptor as high as 100 μM did not alter the ability of heparin to act as a trap for free enzyme (Fig. 12*A*). However, if elongation complexes are formed prior to addition of acceptor template, acceptor-template-dependent stimulation of 3D^{pol}-catalyzed nucleotide incorporation was observed (Fig. 12*B*). In addition, the observed stimulation by acceptor template was concentration-dependent (Fig. 12*B*), saturating in the 10–50 μM range (Fig. 12*C*). Moreover, analysis of products formed in the presence of acceptor template by denaturing PAGE showed that longer products accumulated at a faster rate than in the absence of additional acceptor template (Fig. 13, *cf. − Acceptor and + rA_{30} Acceptor panels*). These effects are not a result of reinitiation as heparin was added along with the acceptor template.

Long products also formed in the absence of additional acceptor template. It is possible that these products are the result of slippage. Alternatively, the rA_{30} in the dT_{15}/rA_{30} primer/template, which is not bound by polymerase, may serve as acceptor template. In order to distinguish between these two possibilities and obtain additional evidence to support template switching, we replaced the oligo$(rA)_{30}$ with oligo$(dA)_{30}$. In Mg^{2+}, dT_{15}/dA_{30} primer/templates do not support poly(rU) synthesis (data not shown), suggesting that oligo$(dA)_{30}$ should not serve as an acceptor template. The template-switching model suggests that a complex comprising 3D^{pol} and nascent chain

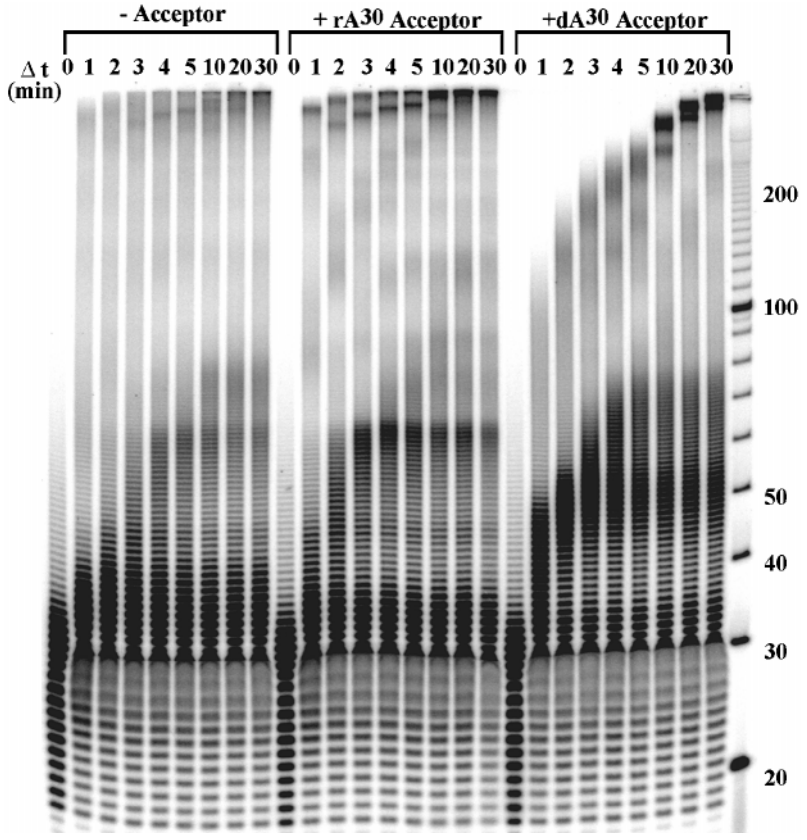

FIG. 13. **Product length is increased by an RNA acceptor template and decreased by a DNA acceptor template.** Reactions were initiated by mixing 3D^{pol} (5 μM), dT_{15}/rA_{30} (10 μM), and [α-^{32}P]UTP (1 μM) and incubated at 30 °C for 3 min, at which time heparin (10 μM), UTP (500 μM), and no acceptor template, rA_{30} acceptor template (100 μM), or dA_{30} acceptor template (100 μM) was added to the reactions such that the final concentrations of 3D^{pol} and dT_{15}/rA_{30} were 0.5 and 1 μM, respectively. After dilution, reactions were quenched at the indicated times (Δt) by addition of EDTA to a final concentration of 50 mM. Products were resolved by electrophoresis on a denaturing 10% polyacrylamide gel. The size of selected bands from the single-stranded, DNA ladder is indicated as a reference.

dissociates from the donor template and binds to the acceptor template. If the destination of the "jumping" complex is dictated by base pairing, then oligo$(dA)_{30}$ might be expected to inhibit formation of long products. In contrast, if slippage synthesis is the mechanism of formation of long products, then oligo$(dA)_{30}$ might be expected to have no effect on formation of long products. As indicated in Fig. 13 (+ *dA_{30} Acceptor panel*), oligo$(dA)_{30}$ inhibited significantly the rate of accumulation of long products. Therefore, we conclude that template switching is the primary mechanism of long product formation in these reactions.

The fraction of complexes formed during the course of the reaction was determined by primer-extension analysis of an end-labeled [^{32}P]dT_{15}/rA_{30} primer/template. The data are shown in Fig. 14. Only 4% of primers were extended, consistent with the steady-state data presented in Table I. This result suggests that all of the nucleotide incorporated derives from a very small fraction of polymerase-primer/template complexes when radioactive nucleotide is used to follow reaction progress. Moreover, the fraction of the extended primers competent for long product formation (*i.e.* products greater than 40 nt in length) represent only 8.7–23% of the total during the course of the 30-min reaction.

DISCUSSION

Although homogeneous, active preparations of poliovirus RNA-dependent RNA polymerase, 3D^{pol}, have been available for several years (5, 6), very little is known about the mechanism of nucleotide incorporation catalyzed by this enzyme. The recent solution of the crystal structure of 3D^{pol} (19) permits structure-function relationships to be defined for this class of polymerase. However, interpretation of effects of mutations in 3D^{pol}-coding sequence on function is compromised greatly by lack of information on the individual steps employed by this enzyme during a catalytic cycle. One reason for this gap is that stoichiometric complexes between 3D^{pol}, primer/template, and nucleotide have yet to be established.

The initial goal of this study was to perform a systematic, quantitative analysis of substrate utilization by 3D^{pol}, thus facilitating the design of a primer/template useful for the elaboration of the minimal kinetic mechanism for single nucleotide incorporation catalyzed by this enzyme. Unlike the DNA-dependent DNA polymerases and reverse transcriptases (22, 23, 32, 35), however, at equilibrium in the presence of excess primer/template all of the poliovirus polymerase in a reaction is not located at a primer/template junction. This conclusion is based on the observation that at least 30% of template nucleotides needed to be coated by primer to observe maximal rates of nucleotide incorporation (Fig. 2). In the case of the Klenow fragment of DNA polymerase I and human immunodeficiency virus reverse transcriptase, a stoichiometry of one 15–20-nt primer/400-1000-nt template can be used without observing any hysteretic effects on the kinetics of nucleotide incorporation (32, 35).

Under conditions of optimal template coating using poly(rA) or poly(rC) as template, differences in activity were observed as the length of primer was varied. Although a 15–20-nt oligo(dT) primer was best for poly(rU) synthesis, a 6-nt oligo(dG) primer was optimal for poly(rG) synthesis. Therefore, the differences in optimal activity as a function of primer length is most likely due to stability of annealed primer/template. This conclusion is further supported by the fact that the predicted T_m value for the best primers is centered around 49 °C (36, 37). Interestingly, T_m values greater than 70 °C, as is the case for dG primers greater than 10 nt in length, decreased significantly the efficiency of nucleotide incorporation. Perhaps, after binding of 3D^{pol} to primer/template, disruption of the duplex is required for efficient initiation of and/or elongation during RNA synthesis. However, regardless of the molecular events governing the differences described above, these differences

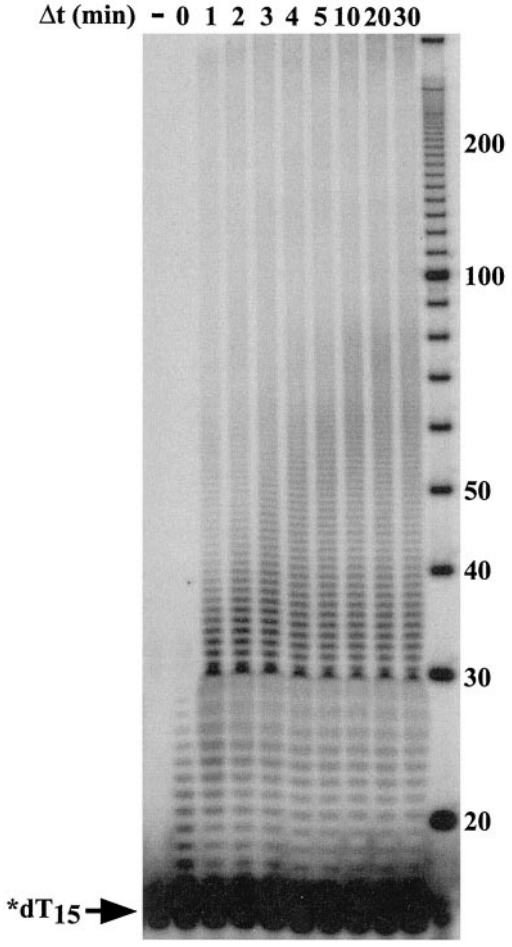

FIG. 14. **Primer extension by 3D^{pol} on dT$_{15}$/rA$_{30}$.** Reaction was initiated by mixing 3D^{pol} (5 μM), an end-labeled [^{32}P]dT$_{15}$/rA$_{30}$ (10 μM) primer/template, and UTP (1 μM) and incubated at 30 °C for 3 min, at which time heparin (10 μM) and additional UTP (500 μM) was added to the reaction such that the final concentrations of 3D^{pol} and dT$_{15}$/rA$_{30}$ were 0.5 and 1 μM, respectively. After dilution, the reaction was quenched at the indicated times (Δt) by addition of EDTA to a final concentration of 50 mM. The *lane* indicated by – is the end-labeled [^{32}P]-dT$_{15}$/rA$_{30}$ primer/template alone. Products were resolved by electrophoresis on a denaturing 10% polyacrylamide gel. The size of selected bands from the single-stranded, DNA ladder is indicated as a reference.

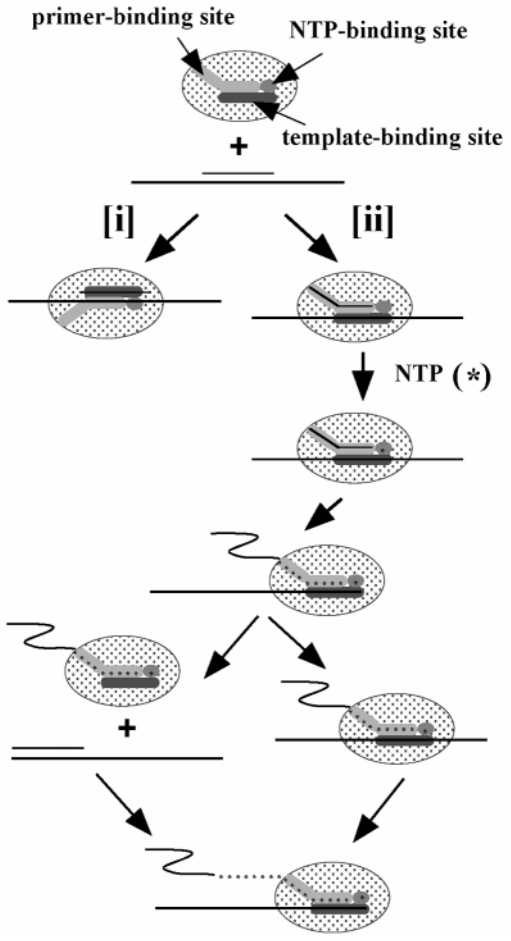

FIG. 15. **Model for 3D^{pol}-catalyzed nucleotide incorporation on homopolymeric primer/templates.** Upon mixing 3D^{pol} and primer/template, one of two possible complexes form. *i*, formation of unproductive complexes. This would include binding of template in the primer-binding site and binding of 3D^{pol} to single-stranded nucleic acid located upstream or downstream of primer. *ii*, formation of "heparin-resistant" complexes capable of slippage synthesis and template switching. The initial binary complex is drawn to reflect a more stable association between 3D^{pol} and primer than 3D^{pol} and template. An increase in formation of this complex might occur by optimizing the stability of the duplex region of primer/template, employing a protein primer, or initiating RNA synthesis *de novo*.

should be considered in the design of heteropolymeric RNA primers for 3D^{pol} and other RdRPs.

In contrast to the pronounced effects on the rate of nucleotide incorporation observed as primer length was varied, effects much less than expected were observed as template length was varied. Under saturating conditions of primer/template and nucleotide, one might expect that as the template length is decreased a proportional reduction in the amount of nucleotide incorporated would occur. This was not observed (Table I) because products greater than unit length were being formed per initiation event during the course of the reaction. The long products did not arise as a result of nucleic acid contamination rather from the primers in the reaction (Fig. 5). By performing reactions in the presence of heparin, a trap for free enzyme (Fig. 8), it was shown that these products formed without enzyme dissociation (Fig. 9). Although slippage may occur to some extent, a template-switching mechanism appears to be the primary mechanism of formation of long products. This conclusion is supported by the finding that the rate and extent of accumulation of products greater than unit length are diminished by dilution (Fig. 11), enhanced by addition of (rA)$_{30}$ acceptor template (Figs. 11–13), and inhibited by (dA)$_{30}$. Although complexes competent to form long products are only a small fraction of the total, these complexes are the primary source of nucleotide incorporated during the course of the reaction (Fig. 14). Taken together, these data are consistent with the model presented in Fig. 15.

The formation of products greater than unit length by polymerases when using templates consisting of "simple" sequences is not novel (30–33). The mechanism of formation of these products, however, appears to differ depending upon the class of polymerase being investigated (30–33). Regardless of the mechanism of formation of long products, the fact that the RdRPs from poliovirus, bovine viral diarrhea virus,[3] and hepatitis C virus[3,4] all share this property is quite important to note. The vast majority of biochemical studies performed to date on these enzymes have evaluated the synthesis of radioactive polymer from radioactive nucleotide and homopolymeric primer/template substrates. Therefore, the results from this

[3] J. J. Arnold and C. E. Cameron, unpublished observations.
[4] R. Bartenschlager, personal communication.

type of analysis may be misinterpreted because a small fraction of enzyme in any reaction gives rise to the greatest fraction of polymerized nucleotide. Mutations in 3D^{pol}-coding sequence that alter the ability of the enzyme to form complexes competent to form long products might appear to have a significant decrease in activity on homopolymeric primer/templates relative to wild-type 3D^{pol} without any substantial change observed in activity on heteropolymeric primer/templates. Therefore, both quantitative and qualitative evaluation of reaction products should always be performed.

Why is such a small fraction of 3D^{pol}-primer/template complexes capable of forming products greater than unit length? This may be related to the fact that complexes which form these products have a very stable association with nascent chain as they are resistant to challenge by heparin. Formation of such stable complexes between polymerase and nascent chain may be similar to those that form with DNA-dependent RNA polymerases (38–40). However, formation of these complexes from a preformed primer/template may require disruption of base pairing between primer and template (Fig. 15, *ii*). This would explain the decrease in nucleotide incorporation as the thermodynamic stability of the primer/template is increased (Fig. 1). *In vivo*, however, RNA synthesis is initiated using protein primer, VPg, which would not present such a dilemma (10). VPg can also be used to initiate RNA synthesis *in vitro* (41). In fact, VPg-primed RNA synthesis on templates similar to those employed here also yields products greater than unit length.[5]

As illustrated in Fig. 15*i*, poliovirus 3D^{pol} that is not competent to form long products has one alternative fate. Given the stochastic nature of 3D^{pol} binding to primer/template and limited ability of the enzyme to recognize specifically a primer/template junction, enzyme is "lost" due to unproductive binding. This contrasts significantly with the biological scenario in which an elaborate array of structured RNA, virus-encoded factors and possibly cellular factors are thought to cooperate in the recruitment of 3D^{pol} to the appropriate site of initiation (11). Of course, the formation of long products in these reactions would sequester enzyme dissociating from the complex in this alternative pathway. Enzyme sequestration probably contributes to the biphasic nature of the kinetics of NMP incorporation (Figs. 3 and 9*A*, for example).

Is there a biological significance to formation of products greater than unit length? In the case of poliovirus, minus-strand RNA synthesis initiates within the A-tract at the 3′ end of genomic RNA (10). As a result, the use of oligo(rA) (and perhaps poly(rA)) as a template may be reasonable. Studies of poliovirus minus-strand RNA have shown that the U-tract at the 5′-end of this RNA is the same length as the A-tract at the 3′-end of genomic RNA (42, 43). If slippage occurred readily in the A-tract, one might expect the expansion of these ends over time. However, this phenomenon has not been reported to date. It is also plausible that the presence of other viral proteins, such as 3AB or 3CD, prevent slippage from occurring.

Our data are most consistent with a template-switching mechanism. Template switching is thought to be the primary mechanism of recombination between viral genomes (44, 45). Furthermore, RNA recombination between viral genomes is thought to be necessary for repair of defective genomes and possibly for the acquisition of new virus-encoded functions (44, 45). In most cases, copy-choice recombination, *i.e.* switching from internal regions, occurs (44, 45). However, in order to repair genomes damaged by the action of ribonucleases, for example, forced-copy-choice recombination, or switching as a result of reaching the end of the template, may be necessary. Whether the template switching described herein reflects a copy-choice or a forced-copy-choice mechanism remains to be determined.

The ability to observe copy-choice recombination between poliovirus genomes in a cell-free system has been demonstrated recently by Kirkegaard (46) and Wimmer (47). Notwithstanding, these experiments utilized a HeLa cell extract, and all of the poliovirus proteins were present. Our results suggest that poliovirus RdRP alone may be sufficient for template switching *in vitro* and, possibly, *in vivo*. Studies employing heteropolymeric donor and acceptor templates should verify that template switching occurs. Furthermore, the use of heteropolymeric substrates should permit the elucidation of the elements of polymerase and nucleic acid required for template switching *in vitro* thus providing greater insight into the mechanism of RNA recombination *in vivo*.

Acknowledgments—We thank Aniko Paul and Eckard Wimmer for providing us with the necessary reagents to initiate our work in this area. We are also grateful to Dr. Kevin Raney and members of the Cameron laboratory for their critical evaluation of the manuscript.

[5] A. V. Paul, personal communication.

REFERENCES

1. Couch, R. B. (1996) in *Fields Virology* (Fields, B. N., Knipe, D. M., and Howley, P. M., eds) Vol. 1, pp. 713–734, Lippincott-Raven Publishers, Philadelphia
2. Houghton, M. (1996) in *Fields Virology* (Fields, B. N., Knipe, D. M., and Howley, P. M., eds) Vol. 1, pp. 1035–1058, Lippincott-Raven Publishers, Philadelphia
3. Buck, K. W. (1996) *Adv. Virus Res.* **47,** 159–251
4. Ishihama, A., and Barbier P. (1994) *Arch. Virol.* **134,** 235–258
5. Plotch, S. J., Palant, O., and Gluzman, Y. (1989) *J. Virol.* **63,** 216–225
6. Neufeld, K. L., Richards, O. C., and Ehrenfeld, E. (1991) *J. Biol. Chem.* **266,** 24212–24219
7. Behrens, S.-E., Tomei, L., and De Francesco, R. (1996) *EMBO J.* **15,** 12–22
8. Lohmann, V., Körner, F., Herian, U., and Bartenschlager, R. (1997) *J. Virol.* **71,** 8416–8428
9. Vázquez, A. L., Martín, J. M., Casais, R., Boga, J. A., and Parra, F. (1998) *J. Virol.* **72,** 2999–3004
10. Rueckert, R. R. (1996) in *Fields Virology* (Fields, B. N., Knipe, D. M., and Howley, P. M., eds) Vol. 1, pp. 609–654, Lippincott-Raven Publishers, Philadelphia
11. Xiang, W., Paul, A. V., and Wimmer, E. (1997) *Semin. Virol.* **8,** 256–273
12. Harris, K. S., Xiang, W., Alexander, L., Lane, W. S., Paul, A. V., and Wimmer, E. (1994) *J. Biol. Chem.* **269,** 27004–27014
13. Andino, R., Rieckhof, G. E., Achacoso, P. L., and Baltimore, D. (1993) *EMBO J.* **12,** 3587–3598
14. Gamarnik, A. V., and Andino, R. (1996) *EMBO J.* **15,** 5988–5998
15. Xiang, W., Cuconati, A., Paul, A. V., Cao, X., and Wimmer, E. (1995) *RNA* **1,** 892–904
16. Hope, D. A., Diamond, S. E., and Kirkegaard, K. (1997) *J. Virol.* **71,** 9490–9498
17. Paul, A. V., Cao, X., Harris, K. S., Lama, J., and Wimmer, E. (1994) *J. Biol. Chem.* **269,** 29173–29181
18. Richards, O. C., and Ehrenfeld, E. (1998) *J. Biol. Chem.* **273,** 12832–12840
19. Hansen, J. L., Long, A. M., and Schultz, S. C. (1997) *Structure* **5,** 1109–1122
20. Tan, K.-L., and Board, P. G. (1996) *Biochem. J.* **315,** 727–732
21. Carroll, S. S., Benseler, F., and Olsen, D. B. (1996) *Methods Enzymol.* **275,** 365–382
22. Benkovic, S. J., and Cameron, C. E. (1995) *Methods Enzymol.* **262,** 257–269
23. Kati, W. M., Johnson, K. A., Jerva, L. F., and Anderson, K. S. (1992) *J. Biol. Chem.* **267,** 25988–25997
24. Reardon, J. E. (1993) *J. Biol. Chem.* **268,** 8743–8751
25. Patel, S. S., Wong, I., and Johnson, K. A. (1991) *Biochemistry* **30,** 511–525
26. Capson, T. L., Peliska, J. A., Kaboord, B. F., Frey, M. W., Lively, C., Dahlberg, M., and Benkovic, S. J. (1992) *Biochemistry* **31,** 10984–10994
27. Flanegan, J. B., and Van Dyke, T. A. (1979) *J. Virol.* **32,** 155–161
28. Pata, J. D., Schultz, S. C., and Kirkegaard, K. (1995) *RNA* **1,** 466–477
29. Lubinski, J. M., Ransone, L. J., and Dasgupta, A. (1987) *J. Virol.* **61,** 2997–3003
30. Falvey, A. K., Weiss, G. B., Krueger, L. J., Kantor, J. A., and Anderson, W. F. (1976) *Nucleic Acids Res.* **3,** 79–88
31. Buiser, R. G., DeStefano, J. J., Mallaber, L. M., Fay, P. J., and Bambara, R. A. (1991) *J. Biol. Chem.* **266,** 13103–13109
32. Huber, H. E., McCoy, J. M., Seehra, J. S., and Richardson, C. C. (1989) *J. Biol. Chem.* **264,** 4669–4678
33. Schlötterer, C., and Tautz, D. (1992) *Nucleic Acids Res.* **20,** 211–215
34. Sankar, S., and Porter, A. G. (1992) *J. Biol. Chem.* **267,** 10168–10176
35. Bryant, F. R., Johnson, K. A., and Benkovic, S. J. (1983) *Biochemistry* **22,** 3537–3546
36. Serra, M. J., and Turner, D. H. (1995) *Methods Enzymol.* **259,** 242–261
37. Sugimoto, N., Nakano, S.-I., Katoh, M., Matsumura, A., Nakamuta, H., Ohmichi, T., Yoneyama, M., and Sasaki, M. (1995) *Biochemistry* **34,** 11211–11216

38. Erie, D. A., Yager, T. D., and von Hippel, P. H. (1992) *Annu. Rev. Biophys. Biomol. Struct.* **21,** 379–415
39. deHaseth, P. L., and Helmann, J. D. (1995) *Mol. Microbiol.* **16,** 817–824
40. deHaseth, P. L., Zupanic, M. L., and Record, M. T., Jr. (1998) *J. Bacteriol.* **180,** 3019–3025
41. Paul, A. V., van Boom, J. H., Filippov, D., and Wimmer, E. (1998) *Nature* **393,** 280–284
42. Yogo, Y., Teng, M.-H., and Wimmer, E. (1974) *Biochem. Biophys. Res. Commun.* **61,** 1101–1109
43. Dorsch-Häsler, K., Yogo, Y., and Wimmer, E. (1975) *J. Virol.* **16,** 1512–1527
44. Jarvis, T. C., and Kirkegaard, K. (1991) *Trends Genet.* **7,** 186–191
45. Nagy, P. D., and Simon, A. E. (1997) *Virology* **235,** 1–9
46. Tang, R. S., Barton, D. J., Flanegan, J. B., and Kirkegaard, K. (1997) *RNA* **3,** 624–633
47. Duggal, R., Cuconati, A., Gromeier, M., and Wimmer, E. (1997) *Proc. Natl. Acad. Sci. U. S. A.* **94,** 13786–13791

Poliovirus RNA-dependent RNA Polymerase ($3D^{pol}$) Is Sufficient for Template Switching *in Vitro*

Jamie J. Arnold and Craig E. Cameron

J. Biol. Chem. 1999, 274:2706-2716.
doi: 10.1074/jbc.274.5.2706
